Regulation of Rabbit Erythrocyte Ca^{2+}-Pump Sensitivity to Calmodulin in Experimental Hyperlipidemia (43916)

B. U. RAESS,[1] R. F. PORRO, AND G. TUNNICLIFF

Departments of Pharmacology, Pathology, and Biochemistry, Indiana University School of Medicine, Evansville, Indiana 47712

Abstract. **Intracellular free calcium activity is in part determined by a calmodulin-regulated plasma membrane Ca^{2+}-pump. Since changes in Ca^{2+} permeability have been implicated in atherosclerotic plaque formation, we initiated a lipid hyperalimentation protocol during which we measured various erythrocyte calcium flux parameters and early atheroma development. Adolescent New Zealand White rabbits were fed a diet with 0.5% cholesterol and 2.5% lard over a 3-month period. Plasma cholesterol and triacylglycerols increased on average 18.7- and 13.9-fold respectively, while erythrocyte membrane cholesterol content decreased 18% and total phospholipids by 54%. After 3 months of lipid hyperalimentation, 22% of the aortic arch was covered with large, early-stage, raised atheroma. Basal and calmodulin-activated (Ca^{2+} + Mg^{2+})-ATPase activities in erythrocyte membranes increased by 31% and 123%, respectively at 2 months, with a concomitant increase in calmodulin affinity (K_m) from 15.6 to 4.2 n*M*. These differences were transient on account of changes in the control animals which exhibited a slowly developing sensitivity to calmodulin during maturation. Basal Ca^{2+} transport and passive Ca^{2+} permeability increased about 7-fold during the hyperlipidemic phase. This suggests that overt hyperlipidemia, leading to atherosclerotic plaque development, alters plasma membrane Ca^{2+} regulatory mechanisms including passive Ca^{2+} permeability. The changes in enzymatic function, membrane composition, and Ca^{2+} permeability seen in this red cell model system may be a reflection of early changes in cells that are directly involved in the development of atherosclerotic plaques.** [P.S.E.B.M. 1995, Vol 209]

Erythrocytes and other mammalian cells actively regulate intracellular Ca^{2+} levels by a calmodulin-activated Ca^{2+}-pump, its biochemical expression being the (Ca^{2+} + Mg^{2+})-ATPase which has been shown to be sensitive to its membranous lipid environment *in vitro* (1–4). It has been proposed that altered Ca^{2+} homeostasis, resulting in an intracellular Ca^{2+} overload, might play an important role in early atherosclerotic plaque formation (5–7). Furthermore, there is a large body of evidence showing that various hyperlipidemias are associated with the pathophysiology of several major cardiovascular diseases including atherosclerosis, particularly large vessel atheroma development (8, 9). Unfortunately, the exact mechanisms through which lipids and calcium are involved in these disease processes are not known.

To address the possible role of Ca^{2+} permeability and the plasma membrane Ca^{2+}-pump in the development of atherosclerosis, we used a progressive/regressive experimentally induced hyperlipidemia rabbit model in which changes in erythrocyte membrane structure and function were followed during atheroma formation. Although most cells, including those of the arterial endothelium, regulate their intracellular Ca^{2+} by a variety of means, the erythrocyte can serve as a useful model system to investigate the contribution of a major regulatory mechanism, specifically, the plasma membrane Ca^{2+}-pump, because it is the only Ca^{2+} regulatory mechanism present (10, 11). The present results support the involvement of diet-induced hyperlipidemia in certain biochemical and

[1] To whom requests for reprints should be addressed at Department of Pharmacology, Indiana University School of Medicine, 8600 University Boulevard, Evansville, IN 47712.

Received October 19, 1994. [P.S.E.B.M. 1995, Vol 209]
Accepted March 23, 1995.

0037-9727/95/2094-0410$10.50/0

structural cellular changes that lead to an altered intracellular Ca^{2+} regulation and may be important in the early development of atherosclerosis.

Materials and Methods

Materials. Crystalline disodium adenosine-5′-triphosphate salt (ATP) was obtained from Boehringer Mannheim, Indianapolis, IN. ^{45}Ca (as $CaCl_2$ in H_2O; avg. specific activity 18.25 mCi/mg) was obtained from Dupont NEN (Boston, MA). Calmodulin, derived from human erythrocytes, and all other chemicals used were obtained from Sigma Chemical Co. (St. Louis, MO).

Animals/Feeding Protocol. Adolescent, male New Zealand White rabbits (1300–1800 g) were obtained from a local breeder and acclimatized for at least 2 weeks on rabbit laboratory chow and water *ad libitum*. Food intake was monitored daily and weights were recorded weekly. At the end of 2 weeks, 5–7 ml of blood was drawn from the marginal ear vein into heparinized tubes, cooled on ice, and used for the various initial baseline measurements. The animals were then randomly divided into control and two experimental groups, each containing three subjects. Over the next 5 days the experimental group was gradually introduced to 180 g/day of another complete, standard rabbit diet that was supplemented with 0.5% cholesterol and 2.5% lard (#7009, Harlan Teklad 0533). The control animals continued to be maintained on the standard rabbit diet. Both experimental groups were fed the diet for 3 months, one group was sacrificed and the second returned to a control diet for an additional 3 months. Fasting blood samples from each animal were collected every 4–6 weeks. At the end of 3 or 6 months the rabbits were injected with heparin (5 mg/kg iv) and 5 min later sacrificed by a sharp blow to the back of the neck. By cutting both carotid arteries, between 40 and 70 ml of blood were collected. Hematocrit values were measured in duplicate by the microtube centrifugation method. Immediately following collection, blood samples were centrifuged at 4°C and 3000 rpm in a refrigerated centrifuge for 10 min, and supernate plasma was removed for lipid analysis.

Erythrocyte Fragility. Erythrocyte fragility was assessed by two methods: (i) Equilibrium osmotic fragility was measured by diluting 25 μl of blood in various NaCl solutions ranging in concentration from 4.09 to 9.00 g/l. After 60 min at room temperature, the mixtures were centrifuged at 2000 rpm and released hemoglobin in the supernate was measured by absorbance spectrophotometry at a wavelength of 540 nm. Fragility is expressed as the extrapolated NaCl (g/l) concentration at which 50% of the cells hemolyze ($A_{50\%} = A_{H_2O} - A_{isot}/2$). (ii) Timed osmotic fragility was measured immediately after blood drawing by diluting 40 μl of blood in 20 ml of a 300 m*M* imidazole solution, pH 7.40 at 25°C with gentle stirring. At 15-sec and 1-min time intervals thereafter up to 10 min, an aliquot of cell suspension was sampled and centrifuged for 10 sec in an Eppendorf microfuge with subsequent removal of the supernate for later determination of released hemoglobin as described above. All measurements were done in duplicate.

Plasma Cholesterol and Triacylglycerols. Total cholesterol plasma concentrations were determined by a method based on that of Allain *et al.* (12) and obtained in kit form from Sigma (Procedure 352). Aqueous bovine cholesterol with 0.1% sodium azide (Sigma C 0534) was used as a standard.

Plasma triacylglycerols (triglycerides) levels were measured by a procedure described by Bucolo and David (13), a kit for which was obtained from Sigma (Procedure 334-uv).

Erythrocyte Ghost Membrane Preparation. A standard, low ionic strength, hemoglobin-depleting membrane preparation, typically used for ATPase activity measurements in human erythrocytes was adapted for rabbits (14). After preparation membranes were reconstituted with 40 m*M* histidine-imidazole to yield a membrane protein concentration of 6–8.5 mg/ml. Membranes were stored on ice for subsequent ATPase assays and phospholipid and cholesterol determinations. Membrane protein concentrations were determined according to the method of Lowry *et al.* (15) using bovine serum albumin as a standard.

Extraction of Lipids from Red Cell Ghost Membranes. This procedure was based on that published by Rose and Oklander (16). Isopropanol (90 μl) was slowly added with gentle mixing to a 20-μl aliquot of membranes and kept on ice for 60 min with occasional agitation. After the addition of 60 μl of chloroform, the mixture was thoroughly mixed and allowed to stand for 60 min before being centrifuged at 700 g for 10 min. The aqueous top layer was then discarded, leaving about 60 μl of the chloroform phase containing extracted lipid.

Determination of Membrane Cholesterol. The chloroform phase was assayed for cholesterol by transferring a 20- to 40-μl aliquot to the enzyme mixture as described for the plasma cholesterol determination using aqueous bovine cholesterol with 0.1% sodium azide (Sigma C 0534) as a standard.

Thin-Layer Chromatographic Separation of Phospholipids. Membrane phospholipids were separated by the procedure of Broekhuyse (17). An aliquot of the chloroform phase, usually 10 μl, was applied to a silica gel 60 plate and developed in a solvent of chloroform, methanol, and ammonium hydroxide (9:5.4:1.1). The plate was dried and developed in a second solvent of chloroform, methanol, acetic acid, and water (9:4:0.6:0.8). After the plate was dried, spots were visualized with iodine vapor and identified

by being compared with a series of standards run at the same time. The standards used were phosphatidylcholine and phosphatidylethanolamine from bovine brain in chloroform, phosphatidylserine from bovine brain and sphingomyelin from bovine erythrocytes, both in a chloroform/methanol (95:5) mixture. All four standards were at a concentration of 10 mg/ml.

Quantitative Assay of Individual Phospholipids. Each spot was scraped from the plate into a tube containing 500 μl of 70% perchloric acid. A glass marble was put on the top and the tube was heated in a 180°C oven for 90 min. After cooling, 4.1 ml of water, 0.2 ml of 5% ammonium molybdate, and 0.2 ml Fiske-Subbarow reagent containing 1-amino-2-naphthol-4-sulfonic acid, sodium sulfite, and sodium bisulfite were added. Tubes were heated for a further 15 min in a water bath at 85°-90°C. The absorbance of the solutions was measured at 830 nm and compared with a P_i standard curve ranging from 4 to 800 ng/ml. This method was based on those described by Böttcher *et al.* (18) and Bartlett (19).

ATPase Assays. (Ca^{2+} + Mg^{2+})-ATPase activities were determined by a semiautomated colorimetric phosphomolybdate complexation method measuring amounts of inorganic phosphate liberated from ATP. Complex formation was measured spectrophotometrically at a wavelength of 750 nm (20).

Inside-Out Vesicle Preparations. Five-milliliter aliquots of blood from animals that were exsanguinated at 3 and at 6 months were washed as described above in five volumes of 154 m*M* NaCl, containing 0.1 m*M* EGTA, pH 7.4 at 4°C. Inside-out vesicularized membrane fragments were prepared according to a method previously published for human erythrocytes (21). Membrane orientation was assessed by the acetylcholinesterase accessibility method of Steck and Kant (22), which yielded an average value of 36% inside-out orientation. Membrane protein was between 3 and 5 mg/ml and estimated as described above.

^{45}Ca Net Uptake into Inside-Out Vesicularized Membrane Fragments. Basic transport incubation medium of 1 ml contained 18 m*M* imidazole, 18 m*M* histidine, 15 m*M* NaCl, 100 m*M* KCl, 3 m*M* $MgSO_4$, 0.1 m*M* ouabain, pH 7.1 and 20 μ*M* $^{45}CaCl_2$ (0.047 mCi/mg), and 200 μg/ml vesicle membrane protein. After the addition of 1 m*M* ATP to start transport, 50 μl aliquots were removed from the stirred incubation vessel at 0, 1, 2, and 3 min and diluted into 60 volumes of an ice-cold stopping solution containing 40 m*M* Tris, 40 m*M* glycylglycine, 0.1 m*M* $MgCl_2$ and 3 m*M* $CaCl_2$, pH 7.1. The quenched vesicles were trapped on a 0.45 μm, 25 mm diameter membrane filter (Gelman, Metrical GA-6) under 15 psi negative pressure. The filters were immersed in a complete counting cocktail and measured in a Beckman LS 7500 scintillation spectrometer. Initial rates of active, ATP-dependent net Ca^{2+} uptake were calculated from the slope of a linear regression fit through the four data points.

Passive Flux or Leakiness Assessment. These experiments were carried out exactly as the uptake measurements described above, but without the addition of ATP.

Morphological Examination. Following exsanguination, the aorta and other tissues were excised and prepared for histomorphological examination in phosphate buffered 10% formaldehyde. The ascending aorta, the aortic arch, thoracic, and abdominal sections of the aorta were excised and cut longitudinally, stained in Sudan red IV and pinned to a support, video-photographed, and digitized. Areas with raised atheroma formations were analyzed morphometrically using Jandel's Mocha software (version 1.0). Aortic segments were paraffin mounted, thin sectioned, and treated with a hematoxylin and eosin stain. Other key tissues such as the heart, pulmonary artery, spleen, liver, kidney, and the adrenals were also collected and preserved in buffered formaldehyde for later histopathological examination.

Statistical Analysis. Significance of differences was calculated using Student's *t* test analysis.

Results

After about 2 weeks on the high lipid diet, animals started to reduce their food intake but continued to gain weight at a rate comparable to that of the control animals. At the end of 3 months, however, their average daily intake was reduced to 54% of that of control animals and they had gained an average of only 416 g, compared with 1050 g for the animals in the control group. The general health and appearance of all animals was good with the exception of one rabbit in the experimental group, which, towards the end of the 3 months on the high lipid diet, showed a slight yellowish discoloration of the ears and the sclera.

Plasma cholesterol and triacylglycerols levels in rabbits that were fed the lipid-supplemented diet markedly increased to a maximum of 3140 ± 906 mg/dl and 568 ± 96 mg/dl, respectively, over the 3-month period (Fig. 1). Three months after discontinuation of the lipid supplementation, both plasma levels had returned essentially to control values.

Atherosclerotic plaque development was assessed morphometrically in the first 4 cm of the aorta including all of the ascending and aortic arch regions and the first part of the descending thoracic aorta. The rabbits in the experimental group exhibited severe, raised, lipid-filled atheroma formations covering about 22% of the 4-cm section of upper aorta. In comparison, animals that were maintained for an additional 3 months on the control diet (i.e., 3 months on the lipid-supplemented diet and 3 months on the matched control diet) had on average 29% of the equivalent aortic

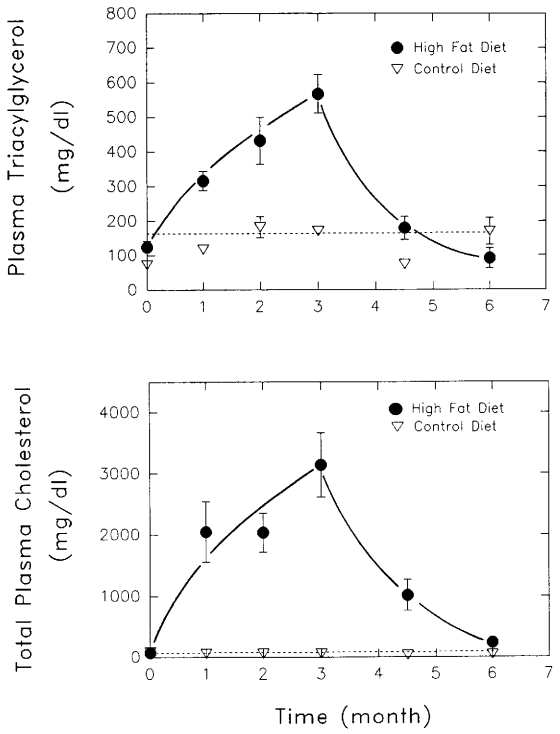

Figure 1. Effects of diet supplementation on plasma lipids. Six-month time course of plasma triacylglycerols (top) and total plasma cholesterol levels (bottom) in control rabbits (▽) and in rabbits on a standard diet supplemented with 2.5% lard and 0.5% cholesterol (●) for the first 3 months, and on the control diet for another 3 months. Error bars are SEM and where missing were smaller than the symbol size.

area covered with lesions. Microscopic examination of visibly raised lesions that were thin sectioned and hematoxylin and eosin stained revealed early atheromatous plaques, in some cases almost as thick as the aortic wall, that were formed by lipid-filled histiocytes. Occasionally, microscopic foci of intimal atheroma were also seen in the abdominal aorta, pulmonary, and coronary arteries but no attempt was made to quantify these lesions. Furthermore, examination of other tissues showed an overall, widespread lipid deposition in the reticuloendothelial system such as lipid-filled histiocytes in the spleen as well as variable degrees of fatty liver. In rabbits maintained on the control diet, no evidence of plaque formation was detected by either gross observation or by microscopic examination in any of the tissues examined.

Erythrocyte membrane cholesterol content in experimental animals decreased by 18% compared with control values during the first 3 months (Table I). Similarly, phosphatidylcholine, phosphatidylethanolamine, phosphatidylserine, and sphingomyelin levels were also decreased. These changes were not reversed during the regressive phase of the study, the molar cholesterol to total phospholipid ratios being 1.16 and 1.12, respectively (control membranes 1.44).

Erythrocyte viability and structural integrity were measured using three different approaches. First, hematocrit values showed a progressive decrease over the period when the animals were maintained on the high-lipid diet. At 3 months, the average hematocrit value was reduced from 45.7% ± 0.7% (n = 6) in control animals to 27.5% ± 1.3% (n = 3) in the lipid-fed group ($P < 0.05$). This decrease was shown to be reversed 6 weeks after the animals were removed from the experimental diet, and at the end of 6 months was back up to 39.6% ± 0.5% (n = 3). At three months, the plasma of several animals actually showed signs of red cell hemolysis. In addition, the osmotic fragility of erythrocytes was assessed by two methods immediately after each blood drawing. Equilibrium osmotic fragility in lipid-fed animals was significantly increased from 4.80 ± 0.16 g/l NaCl producing 50% hemolysis to 5.39 ± 0.16 g/l after 4 weeks, and 5.63 ± 0.09 g/l (n = 3) at the end of 2 months ($P < 0.05$). Similarly, the time to produce 50% hemolysis in erythrocytes exposed to iso-osmotic imidazole (300 mM) was markedly reduced ($P < 0.05$) from an average of 2.68 ± 0.20 min to 1.08 ± 0.48 min (n = 3) after only 4 weeks, and a 64% decrease overall after 3 months of lipid supplementation. This effect was only partially reversible, since after maintenance on the standard diet for an additional 3 months time to half-maximal hemolysis was still decreased by 51% compared with controls.

Table I. Erythrocyte Ghost Membrane Cholesterol and Phospholipid Content[a]

	CHOL	PE	PC	PS	SM
		(μg/mg membrane protein)			
Controls					
1–6 months	37.7 ± 0.7	4.0 ± 0.3	4.5 ± 0.6	1.2 ± 0.2	4.1 ± 0.6
Lipid PRO					
3 months	31.5 ± 1.4[b]	2.0 ± 0.4[b]	2.9 ± 0.7	0.03 ± 0.03[b]	1.8 ± 0.4[b]
Lipid REG					
6 months	31.3 ± 1.2[b]	2.5 ± 0.3[b]	2.70 ± .3	0.1 ± 0.1[b]	1.8 ± 0.2[b]

[a] Values are the mean and SEM from duplicate measurements in three rabbits. Phospholipid amounts are expressed as μgP_i/mg membrane protein. Molar ratios of total cholesterol/phospholipids for the three groups were 1.44, 1.16, and 1.12, respectively. PRO = progressive phase after 3 months on lipid hyperalimentation; REG = regressive phase after an additional 3 months on the control diet; CHOL = cholesterol; PE = phosphatidylethanolamine; PC = phosphatidylcholine; PS = phosphatidylserine; SM = sphingomyelin.

[b] Significantly different from control at $P \leq 0.05$.

Erythrocyte membrane ATPase activities were determined at the beginning, and then every 4 to 6 weeks during the course of the progressive and regressive phase of the 6-month study. Figure 2 shows a gradual but significant ($P < 0.05$) increase in (Mg^{2+})- and ($Na^+ + K^+$)-ATPase activities in animals that were fed the fat and cholesterol supplemented diet and whose plasma lipid levels were elevated. Three months after maintenance on the control diet, these particular activities reverted to close to control values. Basal, calmodulin-independent ($Ca^{2+} + Mg^{2+}$)-ATPase activities appeared to be the least affected, although a small increase in activity from animals on the high lipid diet during the first 2 months could be detected. In contrast to these relatively modest changes in basal activity, maximally calmodulin-stimulated ($Ca^{2+} + Mg^{2+}$)-ATPase activity (0.1 μg/ml calmodulin) (Fig. 2, bottom panel) was markedly increased in erythrocyte membranes from lipid-fed animals and reached a peak at 2 months. Calmodulin-stimulated ($Ca^{2+} + Mg^{2+}$)-ATPase activity in the control group also gradually increased during the course

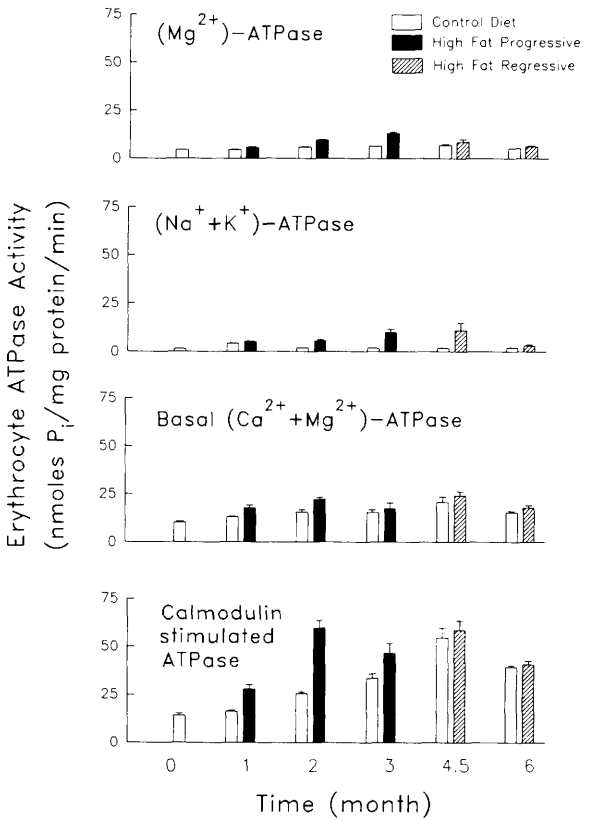

Figure 2. Effects of lipid hyperalimentation on erythrocyte ATPase activities. Various membrane-bound erythrocyte ATPase activities in maturing rabbits on control diets and during the progressive and regressive phase of the lipid hyperalimentation protocol. The concentration of the calmodulin added to the (Ca^{2+}-Mg^{2+})-ATPase (bottom panel) was 0.1 μg/ml. Error bars represent SEM mean from duplicate ATPase determinations from erythrocyte plasma membranes of three to six animals. Where missing, error values were beyond resolution capability.

of the study to the point where there were no significant differences in the calmodulin stimulation at 4.5 and 6 months between the control and experimental groups.

To clarify these observations, full spectrum concentration-effect curves for calmodulin were done. Figure 3 shows calmodulin stimulation of erythrocyte ($Ca^{2+} + Mg^{2+}$)-ATPase activity for both groups of animals at 1, 2, 3, and 6 months of the study. Initially, and even after 1 month, ($Ca^{2+} + Mg^{2+}$)-ATPase activity from animals in the control group showed little responsiveness to the regulatory protein. Over the subsequent course of the study, however, the sensitivity to calmodulin increased, showing a maximal velocity of 39.16 + 0.90 at 1 μg/ml and an apparent K_m of 1.5×10^{-8} *M* by 3 months. Both basal and especially calmodulin-stimulated activities from the experimental animals were increased during the progressive phase of the investigation. This was particularly prominent at 2 months, with an increase in both maximal velocity and apparent affinity (K_m) for calmodulin, the latter of which changed from 15.6 n*M* to 4.2 n*M*. Corroborating the data shown in Figure 2, at 3 months, and especially at 6 months, these differences disappeared.

Basal, initial rate of ATP-dependent, active Ca^{2+} net uptake by inside-out vesicularized membrane fragments from erythrocytes of animals in the lipid-fed group at 3 months was increased more than 6-fold, a stimulation that was completely reversed after animals were removed from the lipid supplemented diet (Fig. 4). This stimulation could not be further increased by the addition of 0.1 μg/ml calmodulin at 3 months, in fact a slight decrease in pump activity is observed. However, the sensitivity to calmodulin was restored after the removal of the lipid supplementation. Passive permeability to Ca^{2+} ("leak") (i.e., net Ca^{2+} uptake by the vesicles in the absence of ATP) was increased markedly in vesicles prepared from erythrocytes of animals after 3 months on lipid supplementation. Similarly to the effects of 3 months of lipid hyperalimentation on basal active transport, this increased passive permeability was restored to control values 3 months after the animals were taken off the high-lipid diet.

Discussion

Excessive levels of intracellular Ca^{2+} are detrimental in both excitable and non-excitable cell types because they severely upset metabolic and structural regulation, including the very processes that are designed to control a typically low, but crucial, free Ca^{2+} concentration ($\approx 10^{-7}$ M). Much credence for this idea comes from investigations showing that Ca^{2+} channel entry blockers are capable of preventing, arresting, and even reversing atherosclerotic plaque formation including the calcific incrustation of extracellular arterial wall components (5, 23–26). Precise control of in-

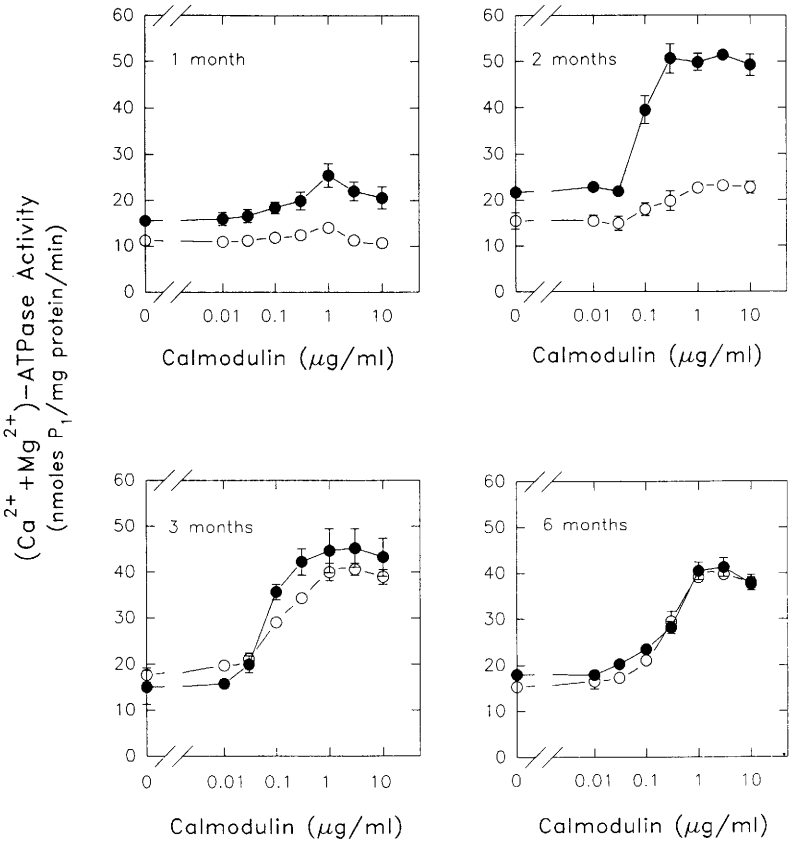

Figure 3. Effects of lipid hyperalimentation on basal and calmodulin-stimulated (Ca^{2+} + Mg^{2+})-ATPase activities. Calmodulin concentration-effect curves in membranes from rabbits on control (○) and lipid-supplemented diets (●) 1, 2, 3, and 6 months after the start of the feeding protocol. (Ca^{2+} + Mg^{2+})-ATPase symbols on the ordinate axis represent basal activities in the absence of any added calmodulin. Error bars represent standard errors of the mean from duplicate ATPase determinations from erythrocyte plasma membranes of three to six animals. Where missing error bars were smaller than symbol size.

tracellular Ca^{2+} regulation depends basically on three main factors: (i) passive transmembrane influx (I_{oi}), (ii) intracellular storage or binding capacity, and (iii) various plasma membrane extrusion mechanisms. Interference with any one of these mechanisms, by a variety of means, will sooner or later lead to a Ca^{2+}-induced cytotoxicosis and cell death. With regard to atherosclerosis, of particular interest are alterations in tissues of the arterial cardiovascular system that might have been brought on by natural senescence, oxidative and mechanical stress, drug induced toxicity, dyslipidemias, and other pathological factors, such as inadequately controlled hypertension and diabetes mellitus.

Since intracellular Ca^{2+} stress and overload, cell death, and calcific incrustation of extracellular structures are prominent ramifications of the atherosclerotic development, it is important to examine the ultimate Ca^{2+} regulatory mechanism (i.e., the plasma membrane Ca^{2+} extrusion pump) under conditions leading to atheroma formation. Although in most cells other mechanisms such as the Na^{+}-Ca^{2+} exchange are present, they have in comparison to the Ca^{2+}-pump a limited capacity and typically depend on a secondary ion concentration gradient. Erythrocytes on the other hand, sharing a common milieu with the arterial endothelial cells, emerge thus as an ideal system to study the Ca^{2+} extrusion pump mechanism in particular. The main reasons for this are: (i) Erythrocyte membranes contain only one transmembraneous extrusion mechanism for Ca^{2+}; (ii) no intracellular Ca^{2+} sequestering mechanisms are present; (iii) both passive and active flux measurements, as well as the biochemical expression of the Ca^{2+}-pump (i.e., the [Ca^{2+} + Mg^{2+}]-ATPase activity) can be determined in a relatively homogeneous cell population. Thus, we chose to study the effects of experimental hyperlipidemia on Ca^{2+} regulatory mechanisms in the well-defined erythrocyte model (26) rather than attempt to use a considerably more complex system such as isolated arterial smooth muscle and endothelial cells where flux measurements typically are difficult to interpret. We believe, moreover, that our approach represents methodologies that could be easily adapted for studying effects of dyslipidemic states in human patients.

The experimental approach and the results presented here with regard to lipid levels, cellular integrity, and atheroma development differ from other studies in that our parameters were monitored over a period of time which allowed the correlation of changes seen in these parameters with concomitant changes in cellular Ca^{2+} regulation. Further, we chose to initiate the study in adolescent animals, as opposed to fully mature animals, as is the case in most investigations. This approach proved useful since there were significant differences found that would have remained elusive if only an endpoint measurement had been made. An example is the case of immediately increased calmodulin sensitivity of the (Ca^{2+} + Mg^{2+})-ATPase ac-

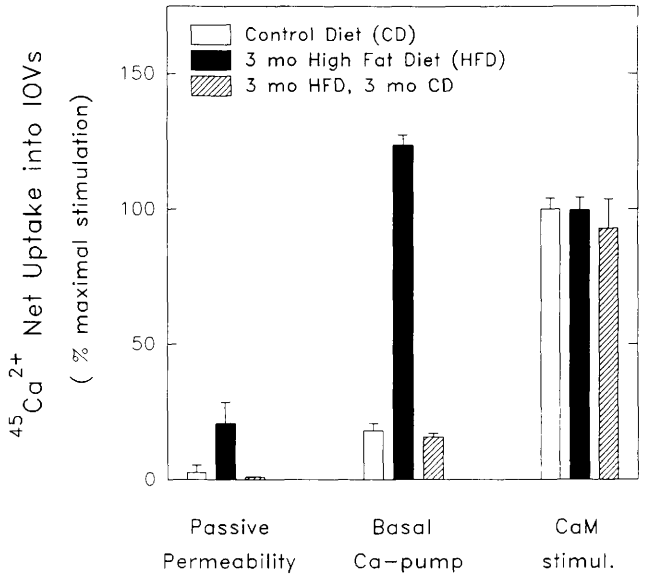

Figure 4. Effects of lipid hyperalimentation on passive Ca^{2+} permeability and active Ca^{2+}-pump rates in inside-out plasma membrane vesicles. Passive permeability represents "leak" into the preparation in the absence of any ATP. Basal Ca^{2+}-pump represents active uptake in the presence of 1 m*M* ATP but no added calmodulin. Calmodulin-stimulated Ca^{2+}-pump represents active uptake in the presence of 1 m*M* ATP and 0.1 μg/ml calmodulin. The data are expressed as normalized values with 100% representing the calmodulin-stimulated pump activity which was 0.615 ± 0.026 nmoles Ca^{2+}/mg IOV protein/min for the control group. Filled bars represent values from animals after 3 months on lipid supplementation and crosshatched bars are from animals that were 3 months on and then 3 months off lipid supplementation. Error bars represent SEM of three independent measurements performed in duplicate.

tivity during the onset of lipid supplementation and, presumably, the development of atheroma formation, a difference from controls which eventually disappeared with time. Two months into the study (i.e., in animals of about 18 weeks of age), there was a marked increase in both maximal velocity and the apparent affinity for calmodulin of the $(Ca^{2+} + Mg^{2+})$-ATPase. The former could be detected as early as 1 month after the beginning of lipid hyperalimentation.

Plasma lipid levels, erythrocyte fragility, and viability as expressed by osmotic fragility and hematocrit values reverted to prehyperalimentation levels during the last 3 months of the study, when the rabbits in the experimental group were receiving control diet. None of the parameters measured, however, with the possible exception of plasma cholesterol and triglyceride levels, reached presupplementation or control levels entirely. Similarly, and of special interest, is the complete reversibility of both passive Ca^{2+} permeability and active vesicular Ca^{2+} uptake, the latter of which is a measure of the active Ca^{2+} extrusion capacity. After three months on the lipid diet, both passive permeability and basal Ca^{2+} uptake by inside-out vesicles were markedly increased, the latter to the point where exogenously added calmodulin could not further activate the rate of uptake. Although the calmodulin-mimicking effect of *in vitro* added acidic phospholipids on the $(Ca^{2+} + Mg^{2+})$-ATPase is a well-documented phenomenon (2, 11, 27, 28), this is to our knowledge a first demonstration of the stimulating effects of *in vivo* lipid supplementation on both $(Ca^{2+} + Mg^{2+})$-ATPase and vesicular Ca^{2+} uptake rates.

The unexpected decrease in erythrocyte membrane cholesterol content from animals on the high-lipid diet is not readily explained. It may be that the concomitant, relatively high triacylglycerol levels interfere with the synthesis/incorporation of cholesterol or bring about an actual displacement of it from the membrane. Furthermore, it is interesting to note that, while several biochemical parameters measured (i.e., various ATPase activities, active and passive Ca^{2+} fluxes, as well as indices of cellular structural integrity such as hematocrit values and osmotic fragility) were for the most part reversible after discontinuing lipid supplementation, we could find no evidence of arresting or inhibiting atheroma formation. Similarly, erythrocyte ghost membrane lipid levels continued to be depressed, while plasma lipid levels were essentially back to presupplementation control values.

From this preliminary study it is clear that in adolescent rabbits lipid hyperalimentation leads both to atherosclerosis and marked changes in cellular Ca^{2+} homeostasis. The latter is observed in both erythrocyte function and viability and may be a reflection of similar changes in cells directly involved in the concomitant atherogenesis. The changes in passive Ca^{2+} permeability seen in erythrocytes from animals in the lipid-fed group appear to be a primary event that can explain the other effects observed in these erythrocytes. It is well established that increased levels of $(Ca^{2+})_i$ are detrimental to normal cell function and viability (29, 30). Our observations with regard to increased osmotic fragility and the presumably linked cell loss in lipid stressed animals corroborates the work by others (31–33) and may well be a direct consequence of the increased "leakiness" of these cells to Ca^{2+}. This same increased permeability to Ca^{2+} is also likely to be the cause of the changes in the Ca^{2+}-calmodulin sensitivity observed. It is noteworthy that in the short term, decreasing plasma lipid levels to prehyperalimentation values, which resulted in normalizing passive membrane permeability properties, but not necessarily lipid composition, does not decrease atherosclerotic plaques in the rabbit aorta.

With our experimental design, it is difficult to rule out direct effects of the lipids and/or changes in erythrocyte lipid composition on the various ATPase activities; however, based on the differences in calmodulin sensitivity of the $(Ca^{2+} + Mg^{2+})$-ATPase seen in Figure 3, we favor the following idea: dietary lipid-induced functional changes (i.e., an increased leak to

Ca^{2+} in erythrocytes and presumably in other cells [including hematopoietic stem cells]) provoke an accelerated senescence at the membrane or the cellular level. This process could lead to altered biochemical properties of the Ca^{2+}-pump (i.e., an increased affinity for calmodulin) and an increase in the total number and turnover of these pumps, thus stimulating enhanced Ca^{2+} extrusion via the plasma membrane Ca^{2+}-pump to meet the increased Ca^{2+} load. This general Ca^{2+} mobilization and turnover could in part explain other cellular changes seen in atherogenesis such as endothelial and intimal smooth muscle cell proliferation, cytokine activation, localized extracellular/interstitial calcium deposition, etc. (5). Considering the apparent importance of a compromised passive Ca^{2+} permeability barrier, which may well be an initial step in the pathophysiologic process, it is clear that this aspect of cellular Ca^{2+} regulation will have to be studied in much greater detail, in model systems, in human dyslipidemic conditions, and directly in cells involved in the development of atherogenesis.

The authors wish to thank Dr. G. K. Matheson and Ms. C. Michel for their expert help with computerized morphometric measurements of aortic segments, and Dr. J. J. Brokaw for assistance with the statistical analysis. We are also grateful for Ms. S. McCormick's and Ms. D. Record's skillful technical assistance.

This work was presented in part at the International Congress of Pharmacology 1994, Montreal, Canada and appears in abstract form in Can J Physiol Pharmacol **72**(1):527, 1994.

1. Roelofsen B, Schatzmann HJ. The lipid requirement of the (Ca^{2+}-Mg^{2+})-ATPase in the human erythrocyte membrane, as studied by various highly purified phospholipases. Biochim Biophys Acta **464**:17–36, 1977.
2. Ronner P, Cazzotti P, Carafoli E. A lipid requirement for the (Ca^{2+} + Mg^{2+})-activated ATPase of erythrocyte membranes. Arch Biochem Biophys **179**:578–583, 1977.
3. Vincenzi FF. Pharmacological modification of the Ca^{2+}-pump ATPase activity of human erythrocytes. Ann NY Acad Sci **402**:368–380, 1982.
4. Delamere NA, Paterson CA, Borchman D, King KL, Cawood SA. Calcium transport, Ca^{2+}-ATPase, and lipid order in rabbit ocular lens membranes. Am J Physiol **260**:C731–C737, 1991.
5. Fleckenstein A, Frey M, Zorn J, Fleckenstein-Grün G. Calcium, a neglected key factor in hypertension and arteriosclerosis. In: Laragh JH, Brenner BM, Eds. Hypertension: Pathophysiology, Diagnosis, and Management. New York: Raven Press, pp471–509, 1990.
6. Strickberger SA, Russek LN, Phair RD. Evidence for increased aortic plasma membrane calcium transport caused by experimental atherosclerosis in rabbits. Circ Res **62**:75–80, 1988.
7. Gleason MM, Medow MS, Tulenko TN. Excess membrane cholesterol alters calcium movements, cytosolic calcium levels, and membrane fluidity in arterial smooth muscle cells. Circ Res **69**:216–227, 1991.
8. Masuda J, Ross R. Atherogenesis during low level hypercholesterolemia in the nonhuman primate. Atherosclerosis **10**:164–177, 1990.
9. Ross R. The pathogenesis of atherosclerosis: A perspective for the 1990s. Nature **362**:801–809, 1993.
10. Schatzmann HJ. Why red cells? In: Raess BU, Tunnicliff G, Eds. The Red Cell Membrane: A Model for Solute Transport. Clifton: Humana Press, pp3–17, 1989.
11. Vincenzi FF. Regulation of the plasma membrane Ca^{2+}-pump. In: Raess BU, Tunnicliff G, Eds. The Red Cell Membrane: A Model for Solute Transport. Clifton: Humana Press, pp123–142, 1989.
12. Allain CC, Poon LS, Chen CS, Richmond W, Fu PC. Enzymatic determination of total serum cholesterol. Clin Chem **20**:470–475, 1974.
13. Bucolo G, David H. Quantitative determination of serum triglycerides by the use of enzymes. Clin Chem **19**:476–482, 1973.
14. Raess BU, Record DM, Tunnicliff G. Interaction of phenylglyoxal with the human erythrocyte (Ca^{2+} + Mg^{2+})-ATPase. Evidence for the presence of an essential arginyl residue. Mol Pharmacol **27**:444–450, 1985.
15. Lowry OH, Rosebrough NJ, Farr AL, Randall RJ. Protein measurement with the Folin phenol reagent. J Biol Chem **193**:265–275, 1951.
16. Rose HG, Oklander M. Improved procedure for the extraction of lipids from human erythrocytes. J Lipid Res **6**:428–431, 1965.
17. Broekhuyse RM. Quantitative two-dimensional thin-layer chromatography of blood phospholipids. Clin Chim Acta **23**:457–461, 1969.
18. Böttcher CJF, Van Gent CM, Pries C. A rapid and sensitive sub-micro phosphorous determination. Anal Chim Acta **24**:203–204, 1961.
19. Bartlett GR. Phosphorous assay in column chromatography. J Biol Chem **234**:466–468, 1959.
20. Raess BU, Vincenzi FF. A semi-automated method for determination of multiple membrane ATPase activities. J Pharmacol Methods **4**:273–283, 1980.
21. Raess BU. Irreversible modification of red cell Ca^{2+} transport by phenylglyoxal. Mol Pharmacol **44**:399–404, 1993.
22. Steck TL, Kant JA. Preparation of impermeable ghosts and inside-out vesicles from the human erythrocyte membranes. Methods Enzymol **31**:172–180, 1974.
23. Henry PD, Bentley KI. Suppression of atherogenesis in cholesterol-fed rabbit treated with nifedipine. J Clin Invest **68**:1366–1369, 1981.
24. Willis AL, Nagel B, Churchill V, Whyte MA, Smith DL, Mahmud I, Puppione DL. Antiatherosclerotic effects of nicardipine and nifedipine in cholesterol-fed rabbits. Arteriosclerosis **5**:250–255, 1985.
25. Kjeldsen K, Stender S. Calcium antagonists and experimental atherosclerosis. Proc Fed Exp Soc Biol Med **190**:219–228, 1989.
26. Raess BU. Pharmacological modification of the red cell Ca^{2+}-pump. In: Raess BU, Tunnicliff G, Eds. The Red Cell Membrane: A Model for Solute Transport. Clifton: Humana Press, pp305–327, 1989.
27. Tokumura A, Mostafa MH, Nelson DR, Hanahan DJ. Simulation of (Ca^{2+} + Mg^{2+})-ATPase activity in human erythrocyte membranes by synthetic lysophosphatidic acids and lysophosphatidylcholines. Effects of chain length and degree of unsaturation of the fatty acid groups. Biochim Biopys Acta **812**:568–574, 1985.
28. Filoteo AG, Enyedi A, Penniston JT. The lipid binding peptide from the plasma membrane Ca^{2+} pump binds calmodulin, and the primary calmodulin-binding domain interacts with lipid. J Biol Chem **267**:11800–11805, 1992.
29. Campbell AK. Intracellular Calcium: Its Universal Role as Regulator. Chichester: Wiley & Sons, pp393–454, 1983.
30. Engelmann B. Calcium homeostasis of human erythrocytes and its pathophysiological implications. Klin Wochenschr **69**:137–142, 1991.
31. Vakakis N, Redgrave TG, Small DM, Castelli WP. Cholesterol content of red blood cells and low-density lipoproteins in hypertriglyceridemia. Biochim Biophys Acta **751**:280–285, 1983.
32. Fröhlich J, Godin DV. Erythrocyte membrane alterations and plasma lipids in patients with chylomicronemia and in Tangier disease. Clin Biochem **19**:229–234, 1986.
33. Vayá A, Martinez M, Carmena R, Aznar J. The lipid composition of red blood cells and their hemorheological behavior in patients with primary hyperlipoproteinemia. Clin Hemorheol **13**:447–457, 1993.